

Ocean Dynamics
Physical-Ecological Response of the California Current System
to ENSO events in ROMS-NEMURO
--Manuscript Draft--

Manuscript Number:								
Full Title:	Physical-Ecological Response of the California Current System to ENSO events in ROMS-NEMURO							
Article Type:	Original Papers							
Keywords:	ENSO composite, CCS, mesoscale, upwelling, bottom-up biophysical interactions							
Corresponding Author:	Nathali Cordero Quiros, Ph.D. University of California San Diego Scripps Institution of Oceanography UNITED STATES							
Corresponding Author Secondary Information:								
Corresponding Author's Institution:	University of California San Diego Scripps Institution of Oceanography							
Corresponding Author's Secondary Institution:								
First Author:	Nathali Cordero Quiros, Ph.D.							
First Author Secondary Information:								
Order of Authors:	Nathali Cordero Quiros, Ph.D. Arthur Joseph Miller Yunchun Pan Lawrence Balitaan Enrique Curchitser Raphael Dussin							
Order of Authors Secondary Information:								
Funding Information:	<table border="1"> <tr> <td>National Oceanic and Atmospheric Administration (NA17OAR4310106)</td> <td>Dr. Nathali Cordero Quiros</td> </tr> <tr> <td>National Science Foundation (OCE1637632)</td> <td>Dr. Nathali Cordero Quiros</td> </tr> <tr> <td>National Science Foundation (OCE1600283)</td> <td>Dr. Nathali Cordero Quiros</td> </tr> </table>		National Oceanic and Atmospheric Administration (NA17OAR4310106)	Dr. Nathali Cordero Quiros	National Science Foundation (OCE1637632)	Dr. Nathali Cordero Quiros	National Science Foundation (OCE1600283)	Dr. Nathali Cordero Quiros
National Oceanic and Atmospheric Administration (NA17OAR4310106)	Dr. Nathali Cordero Quiros							
National Science Foundation (OCE1637632)	Dr. Nathali Cordero Quiros							
National Science Foundation (OCE1600283)	Dr. Nathali Cordero Quiros							
Abstract:	We analyze the bottom-up El Niño/Southern Oscillation (ENSO) driven physical-biological response of the California Current System (CCS) in a high-resolution, "eddy-scale" ocean model with multiple classes of phytoplankton and zooplankton. The response of the SSTa over the CCS is asymmetrical, with La Niña events being more consistently cold than El Niño events are consistently warm, which is in agreement with previous studies. The biogeochemical and ecological response is represented by ENSO-composite anomalies, lag-correlations with an ENSO index, and histograms for ENSO years. The results show lower trophic level interactions during El Niño and La Niña events in which the larger components (diatoms, euphausiids, and copepods) are suppressed in the coastal upwelling zones during El Niño, while the smaller components (flagellates and ciliates) are enhanced. In addition, standing eddies of the CCS modulate the latitudinal structure of the ecological response to ENSO. The results point towards future research to understand how bottom-up changes may lead to variability of patterns in ecological response, including fish populations and top predators.							
Additional Information:								

Question	Response
Is this manuscript (or major parts of it) currently submitted to another journal or has it been submitted before and then either been rejected or withdrawn?	NO

Click here to view linked References

1
2
3
4 ***Physical-Ecological Response of the California Current System***
5
6 ***to ENSO events in ROMS-NEMURO***
7
8
9
10
11

12 ***Authors:***
13
14 *Nathalí Cordero-Quirós¹✉, Arthur J. Miller¹, Yunchun Pan², Lawrence Balitaan²,*
15
16 *Enrique Curchitser³, Raphael Dussin⁴.*
17
18
19
20

21 ¹ *Scripps Institution of Oceanography, University of California, San Diego, USA*
22
23 ² *University of California San Diego, USA*
24
25 ³ *Department of Environmental Sciences, Rutgers University, NJ, USA*
26
27 ⁴ *Geophysical Fluid Dynamics Laboratory, Princeton, NJ, USA*
28
29
30



37 **Abstract**
38
39

40 We analyze the bottom-up El Niño/Southern Oscillation (ENSO) driven physical-
41 biological response of the California Current System (CCS) in a high-resolution, “eddy-scale”
42 ocean model with multiple classes of phytoplankton and zooplankton. The response of the SSTa
43 over the CCS is asymmetrical, with La Niña events being more consistently cold than El Niño
44 events are consistently warm, which is in agreement with previous studies. The biogeochemical
45 and ecological response is represented by ENSO-composite anomalies, lag-correlations with an
46 ENSO index, and histograms for ENSO years. The results show lower trophic level interactions
47 during El Niño and La Niña events in which the larger components (diatoms, euphausiids, and
48 copepods) are suppressed in the coastal upwelling zones during El Niño, while the smaller
49
50
51
52
53
54
55
56
57
58
59
60
61
62
63
64
65

1
2
3
4 components (flagellates and ciliates) are enhanced. In addition, standing eddies of the CCS
5 modulate the latitudinal structure of the ecological response to ENSO. The results point towards
6 future research to understand how bottom-up changes may lead to variability of patterns in
7 ecological response, including fish populations and top predators.
8
9
10
11
12
13

14 **Keywords:** *ENSO composite, CCS, mesoscale, upwelling, bottom-up biophysical interactions*
15
16
17
18

19 ***Declarations***
20
21

22 ***Funding***
23
24

25 This study forms a portion of the Ph.D. dissertation of NCQ, who was partially supported
26 by a UC Mexus CONACYT Fellowship. We thank Prof. Chris Edwards (UCSC) and Dr. Jerome
27 Fiechter (UCSC) for helpful feedback and guidance in understanding NEMURO.
28
29

30 We are grateful to the National Science Foundation (California Current Ecosystem-
31 LTER, OCE1637632, and Coastal SEES, OCE1600283) and the National Oceanic and
32 Atmospheric Administration (NOAA-MAPP; NA17OAR4310106) for funding that supported
33 this research.
34
35

36 ***Conflicts of interest***
37
38

39 *Not applicable*
40
41

42 ***Availability of data and material***
43
44

45 *Not applicable*
46
47

48 ***Code availability***
49
50

51 *Not applicable*
52
53

54 ***Author's contribution***
55
56

57 *Not applicable*
58
59

1
2
3
4 ***1 Introduction***
5
6

7 The California Current System (CCS) is one of the major Eastern Boundary Upwelling Systems
8 (EBUS) in the world e.g., Hickey, 1998; Checkley and Barth, 2009; Miller et al., 2015). The
9 particular dynamics that set up the environment for this highly productive region of the U.S.
10
11 West Coast are under the influence of major climate events such as El Niño Southern Oscillation
12 (ENSO) which remotely imprints variability in coastal upwelling via changes in the main wind
13 patterns (e.g., Schwing et al., 2005; Jacox et al., 2020). These large-scale changes can be well
14 represented by global earth system models but these types of models tend to exhibit large biases
15 in representing the finer-scale dynamics of the EBUS (e.g., Van Oostende et al., 2018; Cordero-
16 Quirós et al., 2019).
17
18
19
20
21
22
23
24
25
26
27
28
29
30

31 In this study we examine the physical-biological response in the California Current to
32 ENSO variability using a high-resolution, “eddy-scale” ocean model that is forced with observed
33 winds. In previous work, we considered the ENSO-forced CCS ecological response in a coarse-
34 resolution climate model (Cordero-Quirós et al., 2019). The high (~7km) resolution here now
35 allows proper representation of upwelling fronts along the irregular U.S. West Coast as well as
36 the generation of an energetic and unstable mesoscale eddy field over realistic topography (e.g.,
37 Marchesiello et al., 2003; Frischknecht et al., 2015). The ecological model here includes two size
38 classes of phytoplankton and three size classes of zooplankton (Kishi et al., 2007; Curchitser et
39 al., 2015), which is more sophisticated than the two size class model of phytoplankton and single
40 size class model of zooplankton ENSO response considered by Cordero-Quirós et al. (2019). The
41 model biogeochemistry, in contrast, is less sophisticated here in that it includes only two
42 nutrients (nitrate and silicate) and excludes the carbonate cycle.
43
44
45
46
47
48
49
50
51
52
53
54
55
56
57
58
59
60
61
62
63
64
65

1
2
3
4
5
6 The basic state of the spatial distributions of phytoplankton communities, and the
7 dependent zooplankton communities that feed on them and each other, establishes
8 biogeographical regions across and along the CCS in the presence of complicated coastline
9 variations and inhomogeneous eddy fields (e.g., Venrick, 2009; Goebel et al., 2013). We
10 consider here how the local physical and ecological response of the CCS is perturbed by ENSO
11 forcing in this context. We focus on individually analyzing the two phytoplankton groups and
12 three zooplankton groups to provide a more fine-scaled view of the bottom-up response of the
13 California Current Ecosystem (CCE) to ENSO compared to less sophisticated coarse-resolution
14 models. The results reveal coherent responses for both warm and cold events, in spite of the
15 mesoscale eddy “noise”, and some interesting and surprising features in the ecology.
16
17
18
19
20
21
22
23
24
25
26
27
28
29
30
31
32
33 We first explain the basic framework of the physical and ecological models. Then we
34 introduce our methods for statistical analyzing the system. We follow that with a presentation of
35 results, and a summary and conclusion section.
36
37
38
39
40
41
42
43 **2 Model Framework**
44
45
46 *2.1 Regional Ocean Circulation Model*
47
48 The physical fields used for this analysis are from a simulation using the Regional Ocean
49 Modeling System (ROMS; Haidvogel et al., 2008; Shchepetkin and McWilliams, 2005). The
50 study domain spans the zonal extent of the CCS, roughly 1200 km offshore, from Vancouver
51 Island (50°N) to southern Baja California (20°N), over a grid with 1/15° (~7 km) horizontal
52 resolution (Van Oostende et al., 2018). The air-sea fluxes are computed using the Coordinated
53
54
55
56
57
58
59
60
61
62
63
64
65

1
2
3
4 Ocean-Ice Reference Experiment (CORE; Griffies et al. 2009) protocol using observed
5
6 reanalysis 6-hourly fields from 1958-2007 for the atmospheric variables and model SST.
7
8 Boundary and initial conditions for temperature, salinity, and velocity are monthly values from
9 the Simple Ocean Data Assimilation (SODA) model output (version 2.1.6), and atmospheric
10
11 forcing is from the Modern Era Retrospective-analysis for Research and Applications (MERRA)
12
13 reanalysis products (Van Oostende et al., 2018). Vertical mixing of momentum and tracers is
14
15 performed along a vertical grid of 50 terrain-following surfaces (Van Oostende et al., 2018).
16
17 Daily model fields were averaged into monthly means for all model variables for the full model
18 time period from Jan 1959 to December 2007. Climatological monthly mean averages were then
19
20 formed and subtracted from the monthly means to obtain 1959-2007 monthly anomalies.
21
22
23
24
25
26
27
28
29
30
31
32
33
34
35
36
37
38
39
40
41
42
43
44
45
46
47
48
49
50
51
52
53
54
55
56
57
58
59
60
61
62
63
64
65

2.2 Ecosystem model

The ecological model is called NEMURO (North Pacific Ecosystem Model for
Understanding Regional Oceanography; Kishi et al., 2007) and was developed by PICES CCCC
(North Pacific Marine Science Organization, Climate Change and Carrying Capacity Program)
as a prototype model to represent the basic trophic structure of the marine ecosystem components
in the North Pacific. This lower trophic level nutrient-phytoplankton-zooplankton-detritus
(NPZD) model has eleven state variables: nitrate (NO_3), ammonium (NH_4), small phytoplankton
(PS), large phytoplankton (PL), small zooplankton (ZS), large zooplankton (ZL), predatory
zooplankton (ZP), silicic acid (Si(OH)_4), and three detrital pools represented by dissolved
organic nitrogen (DON), particulate organic nitrogen (PON), and particulate organic silicate
(Opal). The PS and PL groups use parameters that represent flagellates and diatoms,
respectively. ZP uses parameters that correspond to euphausiids (or krill) that feed on the

1
2
3
4 mesozooplankton group PL (parameters for copepods), the microzooplankton group ZS
5
6 (parameters for ciliates), as well as diatoms (PL). The copepods feed on both the diatoms (PL)
7
8 and the flagellates (PS) as well as the ciliates (ZS). The ciliates (ZS) feed only on the flagellates
9 (PS). The three zooplankton groups were also preyed upon by the modeled sardine and anchovy
10 populations (discussed next). NEMURO uses nitrogen as its primary “currency”, but also
11 includes silicon as a limiting nutrient for diatoms. All the state variables are tracked in units of
12 mmol N m⁻³. The full details and balance equations of NEMURO are given in Kishi et al., 2007.
13
14
15
16
17
18
19
20
21
22
23
24
25

26 **3 Composite analysis method**

27

28 In order to isolate the ENSO signal and remove the impact of long-term trends and
29
30 decadal climate variability, monthly mean anomalies for all ROMS fields were first high-pass
31 filtered using Lanczos method with a cut-off frequency of 10 years, following Cordero-Quirós et
32
33 al. (2019). Identification of El Niño and La Niña years then follows the NOAA protocol
34
35 (NCEP/NOAA,http://origin.cpc.ncep.noaa.gov/products/analysis_monitoring/ensostuff/ONI_v5.php), but only include the moderate-to-strong events and exclude the weak events. In brief, we
36
37 identify El Niño years as those when Niño-3.4 3-month averaged SSTa ≥ 1.0 °C and La Niña
38
39 years as those when SSTa ≤ -1.0 °C, where the anomalies persist during both the fall (SON) and
40
41 winter (DJF) seasons. The composites for each month of the ENSO cycle, from September to
42
43 August over the wintertime peak of each event, were computed using the same method as
44
45 Cordero-Quirós et al. (2019).

46 The years from the ROMS-NEMURO simulation time period included in the 12-month
47
48 El Niño composite are: 1963-1964, 1965-1966, 1968-1969, 1972-1973, 1982-1983, 1986-1987,
49
50
51
52
53
54

1987-1988, 1991-1992, 1994-1995, 1997-1998, and 2002-2003. The resulting years for the La Niña composite are: 1970-1971, 1971-1972, 1973-1974, 1975-1976, 1983-1984, 1984-1985, 1988-1989, 1995-1996, 1998-1999, 1999-2000. That yields a total of 11 El Niño events, and 10 La Niña events.

All of the composite variables were tested for significance using a simple bootstrap test at a 90% significance level and the grid locations where the composite variability is above this threshold are marked with black dots in the figures. Rather than showing all the composite months in the following section, we only focus on key months of the composites and key lag relationships between variables. For this analysis, the nitrate was averaged from 25m to 100m, and the other NPZ model ecological variables were averaged from the surface to 100m.

4. Results

4.1 SST

The SSTa warming of the CCS associated with El Niño events during winter (DJF 3-month composite average), when the ENSO teleconnections peak, is shown in Figure 1 for the ROMS simulation and HadISST observations (Rayner et al., 2003). Composite winter model and observations both show that the warming of the CCS in response to El Niño tends to be significant only along a narrow band along the shore, and the warming signal weakens and becomes cool far offshore. Both the model and observations show the most intense warming off the coast of south Baja California and in the northern portion of the CCS. The near-coastal signature suggests that the response to El Niño is tightly linked to the coastal dynamics controlled by the weakening of the upwelling winds during El Niño that lead to muted upwelling and consequent warming of the SSTa.

1
2
3
4
5
6
7 **Fig. 1** Composite DJF-average of SSTa for El Niño years (*a,b*) and La Niña years (*c-d*) for both ROMS
8 and HadISST observations as indicated on the top right. Significant locations are marked with black dots.
9
10

11 Figure 1 also shows the composite DJF SSTa response of the CCS during cold events
12 associated with La Niña. In contrast with El Niño, La Niña is associated with statistically
13 significant cooling over nearly the entire domain of the CCS. The coldest anomalies tend to be at
14 the southern and northern portions of the CCS, comparable to the patterns shown by El Niño-
15 related SSTa, but they extend further offshore where they are consistently cool. This key
16 difference in the consistency of the offshore response to El Niño and La Niña that is captured by
17 both coarse and fine resolution is not affected by the introduction of mesoscale activity,
18 indicating that its origin lies in the large-scale dynamical response to atmospheric forcing.
19
20
21
22
23
24
25
26
27
28
29
30
31
32
33
34
35
36
37
38
39
40
41
42
43
44
45
46
47
48
49
50
51
52
53
54
55
56
57
58
59
60
61
62
63
64
65

Fig. 2 Histograms of modeled (*a,c,e*) and observed (*b,d,f*) SSTa during a 12-month period from
September through August over the CCS for neutral, El Niño, and La Niña years.

The asymmetry between warm and cold events that was seen in the coarse resolution
model analysis of Cordero-Quirós et al. (2019) also occurs in this high-resolution simulation.
Figure 2 shows the histograms of monthly mean SSTa averaged over the model domain as
captured by the ROMS and observations during a 12-month period from September through
August for warm, cold, and neutral ENSO conditions. The histograms show that in the model
(Fig. 2, left) the SSTa during neutral and El Niño years tend to be relatively symmetric around
the origin, so that cold anomalies also frequently occur during El Niño (only 57% of the SSTa
are positive during warm events). In contrast, the histogram of model SSTa during La Niña
shows a more consistent cooling of the CCS during those years, with much less frequent
occurrences of warm months (67% of SSTa are cold). Observations are generally consistent with

1
2
3
4 the asymmetry of the model histograms, with 55% of El Niño event anomalies being warm and
5 64% of the La Niña anomalies being cool. But observations also exhibit stronger anomalies in
6 7 the histograms. For example, observed neutral years appear to be strongly ‘tailed’ towards warm
8 events, a feature that is not captured by the model. These differences may suggest possible model
9 10 biases, be due to the mismatch of air-sea coupling on the eddy scale due to the forcing protocol
11 12 (e.g., Seo et al., 2016), or be associated with the random mesoscale activity that occurs
13 14 differently in the model and observations. Overall, these results further confirm the asymmetrical
15 16 response of the CCS in which La Niña events are associated with a more consistent cooling than
17 18 El Niño events are associated with consistent warming (cf., Fiedler and Mantua, 2017), even
19 20 though El Niño is associated with the most extreme warm SSTa events (e.g., McGowan et al.,
21 22 1998).
23
24
25
26
27
28
29
30
31
32
33
34 *4.2 Lower trophic level response*
35
36 We next explored the relationship of the nutrients, phytoplankton and zooplankton fields
37 to the changes in ENSO conditions. Nitrate and small phytoplankton show a coherent response in
38 winter but all of the ecological fields showed their largest and most significant ENSO response
39 40 in the spring season when their seasonal bloom occurs. This is in contrast to the physical
41 42 response that peaks significantly in late winter after the atmospheric teleconnection forcing has
43 44 generated its largest oceanic signal. Rather than showing the composite maps of all the
45 46 ecological variability, for brevity we first show the map for JFM 3-month composite average
47 48 anomalies of nitrate (which is also representative of the spring), and then present the lagged
49 50 correlation between the wintertime ENSO index (ONI) and the springtime ecological response.
51
52
53
54
55
56
57
58
59
60
61
62
63
64
65

1
2
3
4 The structures seen in these correlation maps are very similar to those seen in the various
5 composite maps, which are remarkably persistent from month to month in the spring.
6
7
8
9
10
11
12
13
14

15
16
17 **Fig. 3** Composite JFM-averaged anomalies of vertically averaged (25m to 100m) NO_3 for El Niño (left)
18 and La Niña (right) years. Locations where composite response is significant are marked every 5 grid
19 points (black dots).
20
21
22
23
24
25
26
27
28
29
30
31
32
33
34
35
36
37
38
39
40
41
42
43
44
45
46
47
48
49
50
51
52
53
54
55
56
57
58
59
60
61
62
63
64
65

4.3 Composite variability of NO_3

The biogeochemical response of the CCS during warm and cold events is succinctly represented by composite anomalies of nitrate (NO_3) concentrations in the water column (averaged from 25 to 100 m) during JFM. Similar results hold for the silicate field. Figure 3 shows that the composite vertically averaged anomalies of NO_3 in the model captures the nutrient depleted conditions along the coast due to muted coastal upwelling during El Niño, and nutrient enhancement due to stronger upwelling during La Niña. The spatial distribution of ENSO-related composite NO_3 anomalies is confined to a roughly 500km region along the coast, with more patchy structure offshore during both warm and cold events. Unlike composite SSTa, the composite anomalies of NO_3 are quite symmetric over the CCS in both their spatial pattern and significance, except for slight differences off Southern California Bight and Baja California. The upwelling-driven response of the NO_3 in the water column may be further amplified by changes in the biogeochemistry of the source waters (Rykaczewski and Dunne, 2010; Bograd et al., 2015) but further research is necessary to address this issue.

4.4 Lagged correlation of lower trophic levels with the ONI

Figure 4 shows the 3-month lagged correlation between January ONI values and April anomalies of the ecological fields in NEMURO. Positive values (red) indicate that biomass

1
2
3
4 anomalies during April over the CCS are in phase with the SSTa in January over the tropical
5 Pacific. During El Niño conditions over the CCS when upwelling favorable winds tend to be
6 weaker, the nutrient supply to the photic zone decreases, as shown by the negative lagged-
7 correlations of vertically averaged NO_3 (which is similar to the silicate fields) along the coastal
8 region. As a consequence of the nutrient-depleted waters, large phytoplankton (diatoms, Fig. 4-c)
9 biomass decreases along the coastal band and in patchy areas offshore. The response of the
10 predatory zooplankton (krill, Fig. 4-f) and mesozooplankton (copepods, Fig. 4-e) that each graze
11 partly on diatoms resembles this diatom field. The predatory zooplankton has a stronger
12 correlative response to ONI than mesozooplankton since it preys upon the now-reduced field of
13 mesozooplankton. Thus, the larger components of the food web respond as expected with
14 reductions in biomass for El Niño conditions and enhancements for La Niña conditions.
15
16
17
18
19
20
21
22
23
24
25
26
27
28
29
30
31
32
33
34
35
36
37
38
39
40
41
42
43
44
45
46
47
48
49
50
51
52
53
54
55
56
57
58
59
60
61
62
63
64
65

Fig. 4 Lagged correlation of ecological fields during April with January of the Oceanic Niño Index (ONI). Locations where correlations are >95% confidence level are marked with black dots.

In contrast, along the coastal region Figure 4 shows that positive anomalies of small phytoplankton (flagellates, Fig. 4-b) biomass occur during warm event conditions (positive ONI). This is consistent with smaller phytoplankton cells having lower nutrient requirements and more effective uptake, which gives them competitive advantage over larger cells (diatoms) under low nutrient conditions (Van Oostende et al., 2018; Edwards et al., 2012). Small zooplankton (ciliates, Fig. 4-d) also increases in these near-coastal areas, both due to the enhancement of its only food source (the flagellates) and to the reductions in both of its predators (euphausiids and copepods). Figure 4 clearly shows that NEMURO captures this kind of ecosystem dynamics where the smaller phytoplankton groups thrive under lower nutrient conditions nearshore due to muted upwelling during El Niño. This type of response to El Niño, where there are winners in

1
2
3
4 the smaller components of the food web near the coast, is an unexpected result of our analysis
5 and shows the efficacy of adding more complexity to the food web compared to more simplistic
6 ecological models.
7
8
9
10
11
12
13

14 Another interesting feature of the ecological correlation maps (and seen consistently in
15 the month-to-month composite response as well, as in Figure 3) is the occurrence of ecological
16 anomalies locked spatially around standing eddies (also called permanent meanders or stationary
17 waves) in the simulated California Current. These have been previously discussed for the
18 physical fields of currents and sea level (Marchesiello et al., 2003; Centurioni et al., 2008), but
19 we have not noticed this type of response being linked so clearly to the ecology, especially in the
20 context of modulation of the ecological fields by ENSO. Figure 5 shows the mean sea-level
21 height field over the entire period of our simulation. Its meandering structure is consistent with
22 what was previously found by Centurioni et al., (2008) for a shorter-term mean of the SSH field
23 from ROMS. The large-scale standing eddies (roughly four-to-five of them, undulating north-
24 south along the CCS) are climatologically locked to major capes and bathymetric features and
25 can also be associated with local enhancements of the mesoscale eddy field.
26
27
28
29
30
31
32
33
34
35
36
37
38
39
40
41
42
43
44
45

Fig. 5 Long term mean of sea surface height (SSH) from the ROMS monthly fields from 1959 to 2007.

50 We looked with more detail into this persistent mesoscale structure of the CCS in ROMS
51 by analyzing composites of sea surface height anomalies (SSHa) during winter for El Niño and
52 La Niña events. Fig. 6 shows that a consistent rise in sea level occurs during El Niño and a
53 consistent lowering of sea level occurs during La Niña all along the coastal region of the CCS.
54
55 This implies a large-scale weakening of the surface California Current during El Niño and a
56
57
58
59
60
61
62
63
64
65

strengthening of the surface current during La Niña. This can be caused by both thermal expansion effects and dynamically driven thermocline depth changes associated with CCS ENSO anomalies. The patterns of eddy structures seen throughout the coastal regions in Fig. 6, however, are not consistently localized around the standing eddies of Fig. 5 and they do not occur with opposite signs for warm and cold conditions. This suggests that the large-scale forcing from the atmosphere modulates the mean state of the CC during ENSO events, rather than by consistently changing the local mesoscale eddy dynamics around the persistent meanders in this simulation. Additional dynamical analysis will be required in future work to confirm this interpretation.

The positive composite anomalies of vertically averaged NO_3 for JFM in Fig. 3 are consistent with the composite negative anomalies of the SSH field during January along the coast during La Niña (Fig. 6, right). Likewise, the composite response to El Niño, which is stronger than the La Niña response, is also consistent with the simulated negative anomalies of vertically averaged NO_3 .

Fig. 6 Composite anomalies of the ROMS sea surface height (SSH_a) for El Niño (left) and La Niña (right) events.

The north-south spatial distribution of composite NO_3 anomalies is much more similar to the mean state of SSH (Fig. 5), as it clearly follows its climatological meanders, than to any of the eddy structures seen in Fig. 6. This suggests that variability of NO_3 during El Niño and La Niña events is affected by large-scale changes in the upwelling favorable winds that modulate the

background state. The persistent meanders might be channels for filament ejection of biomass from coastal regions, whereby strong production near the coast is transported offshore by the eddies or the mean flow. This result needs to be further explored in future work to establish the dynamical drivers of the structures of the ecological response and its modulation by ENSO. Additional research is also necessary to better elucidate how potential variability of the mesoscale field derived from ENSO can be modulated by the background flow.

4.5 Probability distribution of ecological fields over the CCS

In order to address differences in the consistency of the ecological response of the CCE to cold and warm events, we computed histograms of the ecological fields in NEMURO over a coastal swath from 22°N to 48°N extending roughly 300 km offshore, which is the region of strongest response to ENSO seen in the composites. The histograms of NO₃ anomalies show a fairly consistent depletion during El Niño years with fairly consistent enhancement of NO₃ during La Niña (Figure 7). Negative anomalies represent 71% of the total distribution for El Niño years, and 77% of the anomalies are positive for La Niña years, which is much more symmetric than found for the SSTa histograms.

Fig. 7 Histograms of anomalies of vertically averaged NO₃, biomass of small phytoplankton, and diatoms, during a 12-month period from September through August over a coastal swath of ~300 off-shore from 22°N to 48°N. Anomalies are shown for neutral years (a,b,c), El Niño (d,e,f) and La Niña (g,h,i) and are expressed in units of mmol N m⁻³.

Histograms for diatoms, in contrast, have more consistency during cold events, with 70% of negative anomalies during La Niña and 59% of positive anomalies during El Niño (Figure 7). The ciliates, however, are less consistently altered (Figure 7) than diatoms for both warm (49%) and cold events (57%) indicative of their narrower coastal response and higher signals in the

1
 2
 3
 4 high latitudes (see Figure 4). The distribution for predatory zooplankton (Figure 8) is less
 5 consistent than for diatoms, with El Niño (La Niña) events having 64% (70%) of their associated
 6 anomalies on the negative (positive) side of the distribution. Similar results hold for the copepod
 7 distributions (50% vs. 69%). And the ciliates reflect the flagellate distribution (47% vs. 63%) but
 8 with a stronger consistency during La Niña events. The percentage of cold and warm anomalies
 9 associated to each event for every ecological group and SST are summarized in Table 1. In
 10 general, the histograms of the biological fields in NEMURO do not exhibit such a strong
 11 asymmetry as that associated with SSTa. This suggests more complicated dynamics that go
 12 beyond a linear response to wind variability imprinted by ENSO teleconnections.
 13
 14
 15
 16
 17
 18
 19
 20
 21
 22
 23
 24
 25
 26
 27
 28

29 **Fig. 8** Histograms of anomalies of biomass for small zooplankton, large zooplankton, and predatory
 30 zooplankton during a 12-month period from September through August over a coastal swath of ~300 off-
 31 shore from 22° N to 48° N. Anomalies are shown for neutral years (*a,b,c*), El Niño (*d,e,f*) and La Niña
 32 (*g,h,i*) and are expressed in units of mmol N m^{-3} .
 33
 34
 35
 36

37 **TABLE 1:** Percentage of warm anomalies during El Niño years (second column) and of cold
 38 anomalies during La Niña years (last column) for ecological variables and SST.
 39

	EN<0 (%)	LN>0 (%)
NO₃	71	77
PS	49	57
PL	59	70
ZS	47	63
ZL	58	69
ZP	64	70
SST ROMS	57	67
SST	55	64
HadISST		

1
2
3
4 **5. Summary and Conclusion**
5
6
7
8
9
10
11
12
13
14
15
16
17
18
19
20
21
22
23
24
25
26
27
28
29

We analyzed the bottom-up ENSO-driven physical-biological response of the CCS and the CCE in a high-resolution, “eddy-scale” ocean model with two classes of phytoplankton and three classes of zooplankton. The physical oceanographic responses in SSTa exhibited asymmetries similar to those in the coarse resolution model found by Cordero-Quirós et al. (2019), with La Niña events being more consistently cold than El Niño events are consistently warm (Figures 1 and 2). We used a statistical analysis strategy involving composites, lag correlations, and histograms to assess the ENSO-forced biogeochemical and ecological response (Figures 3-5). We found that the larger components (diatoms, euphausiids and copepods) are suppressed in the coastal upwelling zones during El Niño, while the smaller components (flagellates and ciliates) are enhanced.

30
31
32
33 Most observational studies of the ecological response to ENSO in this region aggregate
34 phytoplankton and zooplankton, so it is unclear how realistic this simulation is. In general,
35 chlorophyll is often used as a proxy for phytoplankton biomass. This approach facilitates
36 comparison with satellite observations of chlorophyll (e.g., Thomas et al., 2012). The type of
37 algorithms that are used for chlorophyll computation involve variables that are unique to each
38 phytoplankton size-class, e.g., grazing and mortality rates, and saturation constants for nutrient
39 uptakes. Thus, using chlorophyll as a proxy for phytoplankton biomass may provide a overall
40 broad-brush view of the response of the ecosystem to ENSO, but the complexity of its
41 calculation can obscure the interesting ecological dynamics at lower trophic levels.
42
43
44
45
46
47
48
49
50
51
52
53
54

55 The dichotomy in the details of the simulated bottom-up response of the CCE to ENSO
56 (Fig. 4) motivates us to identify interactions between the lower trophic levels. When El Niño
57
58
59
60
61
62
63
64
65

1
2
3
4 drives nutrient depletion in the photic zone due to suppressed upwelling, the larger
5 phytoplankton (diatoms) has less nutrients available for their uptake and growth, resulting in
6 decreased biomass. It is unclear whether the decrease in diatoms biomass is dominated by
7 mortality or by reduced size as a consequence of nutrient limitation, but future research could
8 analyze the changes in opal detrital pool in order to address this question. Small phytoplankton is
9 more resilient to nutrient depletion since its size allows for smaller nutrient concentrations, and
10 at the same time they face less competition from diatoms for nutrients. During La Niña,
11 intensified upwelling brings nutrients to the photic zones favoring phytoplankton populations,
12 particularly the larger ones with more capacity for uptake. Once more, competition comes into
13 play, and small phytoplankton is reduced under upwelling favorable conditions.
14
15
16
17
18
19
20
21
22
23
24
25
26
27
28
29
30

31 The results also show that vertically averaged concentrations of NO_3 in the water column
32 increase in response to intensified upwelling during La Niña and decrease as a consequence of
33 weaker upwelling during El Niño (Figs. 3-4). If we consider the alongshore winds stress along
34 the CCS to be the primary driver of coastal upwelling and consequent nutrient supply, one could
35 expect the NO_3 response to be as asymmetrical as the SSTa. However, the lack of this
36 asymmetry suggests that other dynamics come into play when determining the ENSO related
37 variability of NO_3 . The supply of nutrients to the photic zone is also determined by subsurface
38 ocean variability e.g., pycnocline depth and chemical properties of the source waters. Future
39 analysis of the subsurface conditions is necessary to understand the local and advective changes
40 that impact the supply of NO_3 into the photic zone, and how these conditions change in response
41 to ENSO.
42
43
44
45
46
47
48
49
50
51
52
53
54
55
56
57
58
59
60
61
62
63
64
65

1
2
3
4 The high resolution of the regional circulation model accounts for the many interesting
5 effects of mesoscale eddy features that drive variability in the EBUS like the CCS. For example,
6 we noted a fascinating structure in the ecological response that is linked to the latitudinal
7 structure of the standing eddies, and possibly the mesoscale eddy distribution, locked into the
8 CCS. This response structure is clearly evident in the composites and in the correlation maps
9 (Figs. 3 and 4, respectively), which suggests a linear modulation of the background flow fields
10 between El Niño and La Niña events. It is still unclear how the mesoscale features of the CCS
11 influence the variability of the biogeochemical properties of the CCE, and how this may further
12 impact the spatial distribution of phytoplankton and zooplankton communities, both under
13 normal conditions and during ENSO events. Further work is needed in this regard.
14
15
16
17
18
19
20
21
22
23
24
25
26
27
28
29
30

31 In conclusion, the results of this work show that a simple lower trophic level NPZD
32 model like NEMURO is a useful tool to represent the bottom-up ENSO related response of the
33 CCE in ROMS. Patterns of fish migration highly depend on the regions of high nutrient
34 concentration, and fish catch is strongly related to high chlorophyll coastal regions (Stock et al.,
35 2017). Shedding light on these dynamics will help us better address the future changes of habitat
36 of fish populations like sardine and anchovy, as well as top predators, as a response of changes in
37 their environmental modulators on seasonal, interannual and global-warming timescales.
38
39
40
41
42
43
44
45
46
47
48
49
50
51

52 **Acknowledgements**

53 This study forms a portion of the Ph.D. dissertation of NCQ, who was partially supported
54 by a UC Mexus CONACYT Fellowship. We thank Prof. Chris Edwards (UCSC) and Dr. Jerome
55 Fiechter (UCSC) for helpful feedback and guidance in understanding NEMURO.
56
57
58
59
60
61
62
63
64
65

1
2
3
4
5
6 We are grateful to the National Science Foundation (California Current Ecosystem-
7
8 LTER, OCE1637632, and Coastal SEES, OCE1600283) and the National Oceanic and
9
10 Atmospheric Administration (NOAA-MAPP; NA17OAR4310106) for funding that supported
11
12 this research.
13
14

15
16 **References**
17

18
19 Bograd, S.J., Pozo Buil, M., Du Lorenzo, E., Castro, C.G., Shroeder, I.D., Goericke, R.,
20 Andersson C.R., Benitez-Nelson, C., Whitney, F.A., 2015. Changes in source waters to the
21 Southern California Bight. Deep Sea Res. 112, 42-52.
22 <https://doi.org/10.1016/j.dsr2.2014.04.009>
23
24
25 Centurioni, L.R., Ohlmann, J.C., Niiler, P.P. 2008. Permanent meanders in the California Current
26 System. J. Phys. Oceanogr. 38, 1690–1710.
27
28 Checkley, D.M., Barth, J.A., 2009. Patterns and processes in the California Current
29 System. Prog. Oceanogr. 84, 49–64.
30
31
32
33 Cordero-Quirós, N., Miller, A.J., Subramanian A.C., Luo, J.Y., Capotondi, A., 2019. Composite
34 physical-biological El Niño and La Niña conditions in the California Current System in
35 CESM1-POP2-BEC. Ocean Modelling, 142, 101439.
36 <https://doi.org/10.1016/j.ocemod.2019.101439>
37
38
39 Curchitser, E.N., Haidvogel, D.B., Hermann, A.J., Dobbins, E.L., Powell, T.M., Kaplan, A.,
40 2005. Multi-scale modeling of the North Pacific Ocean: assessment and analysis of simulated
41 basin-scale variability (1996–2003). J. Geophys. Res. 110.
42 <https://doi.org/10.1029/2005JC002902>
43
44
45 Edwards, K.F., Thomas, M.K., Klausmeier, C.A., Litchman, E., 2012. Allometric scaling and
46 taxonomic variation in nutrient utilization traits and maximum growth rate of phytoplankton.
47 Limnol. Oceanogr. 57, 554–566. <https://doi.org/10.4319/lo.2012.57.2.0554>.
48
49
50
51
52 Fiechter, J., Rose, K. A., Curchitser, E. N., Hedstrom, K. S. 2015. The role of environmental
53 controls in determining sardine and anchovy population cycles in the California Current:
54 Analysis of an end-to-end model. Progress in Oceanography, 138, 381–398.
55 <https://doi.org/10.1016/j.pocean.2014.11.013>
56
57
58
59
60
61
62
63
64

1
2
3
4 Fiedler, P.C., Mantua, N.J., 2017. How are warm and cool years in the California Current related
5 to ENSO? *J. Geophys. Res. Oceans* 122 (7), 5936–5951.
6 <http://dx.doi.org/10.1002/2017JC013094>.
7
8
9 Frischknecht, M., M. Munnich., Gruber, N. 2015. Remote versus local influence of ENSO on the
10 California Current System. *J. Geophys. Res. Oceans*, 120, 1353-1374
11
12 Goebel, N.L., Edwards, C.A., Zehr, J.P., Follows, M.J., Morgan, S.G. 2013. Modeled
13 phytoplankton diversity and productivity in the California Current System. *Ecol. Model.* 264
14 (2013) 37-47.
15
16 Griffies, S., Biastoch, C., Bryan, F., Danabasoglu, G., Chassignet, E.P., England, M.H., Gerdes,
17 R., Haak, H., Hallber, R.W., Hazeleger, W., Jungclaus, J., Large, W.G., Madec, F., Pirani,
18 A., Samuels, B., Sheinert, M., Gupta, A.S., Severijns, C.A., Simmons, H.L., Treguier, A.M.,
19 Winton, M., Yeager, S., Yin, J., 2009. Coordinated ocean-ice reference experiments (CORE).
20 *Ocean Model.* 26, 1–46.
21
22
23
24 Haidvogel, D.B., Arango, H., Budgell, W.P., Cornuelle, B.D., Curchitser, E., DiLorenzo, E.,
25 Fennel, K., Geyer, W.R., Hermann, A.J., Lanerolle, L., Levin, J., McWilliams, J.C., Miller,
26 A.J., Moore, A.M., Powell, T.M., Shchepetkin, A.F., Sherwood, C.R., Signell, R.P., Warner,
27 J., Wilkin, J., 2008. Regional ocean forecasting in terrain-following coordinates: model
28 formulation and skill assessment. *J.Comput. Phys.* 227, 3595–3624.
29
30
31
32 Hickey, B.M., 1998. Coastal oceanography of western North America from the tip of Baja
33 California to Vancouver Island. In: Robinson, A.R., Brink, K.H. (Eds.), *The*
34 *Sea, The Global Coastal Ocean: Regional Studies and Syntheses*. J. Wiley and
35 Sons Inc, New York, pp. 345–391.
36
37
38
39 Kishi, M.J., Kashiwai, M., Ware, D.M., Megrey, B.A., Eslinger, D.L., Werner F.E., Noguchi-
40 Aita, M., Azumaya, T., Fuji, ., Hashimoto, S., Huang, D., Izumi, H., Ishida, Y., Kang, S.,
41 Kantakov, G.A., Kim, H., Komatsu, K., Navrotsky, V.V., Smith, S.L., Tadokoro, K., Tsuda,
42 A., Yamamura, O., Yamanaka, Y., Yokouchi, K., Yoshie, N., Zhang, J., Zuenko, Y.I.,
43 Zvalisnky, V.I. 2007. NEMURO—a lower trophic level model for the North Pacific marine
44 ecosystem. *Ecol. Model.* 202, 12–25.
45
46
47 Marchesiello, P., McWilliams, J.C., Shchepetkin, A., 2003. Equilibrium structure and dynamics
48 of the California Current system. *Journal of Physical Oceanography* 33 (4), 753–783.
49
50
51 McGowan, J.A., Cayan, D.R., Dorman, L.M., 1998. Climate-ocean variability and ecosystem
52 response in the northeast Pacific. *Science* 281, 210–217.
53
54
55 Miller. A.J., Song, H., Subramanian, A.C., 2015. The physical oceanographic environment
56 during the CCE-LTER Years: Changes in climate and concepts. *Deep-Sea Res.* 112, 6-17.
57
58
59
60
61
62
63
64

1
2
3
4 Politikos, D.V., Curchitser, E.N., Rose, K.A., Checkley D.M., Fiechter, J., 2017. Climate
5 variability and sardine recruitment in the California Current: A mechanistic analysis of an
6 ecosystem model. *Fisheries Oceanography* 27, 602-622. DOI: 10.1111/fog.12381
7
8

9 Rayner, N.A., Parker, D.E., Horton, E.B., Folland, C.K., Alexander, L.V., Rowell, D.P.,
10 2003. Global analyses of sea surface temperature, sea ice, and night marine
11 air temperature since the late nineteenth century. *J. Geophys. Res.* 108, 4407.
12 <http://dx.doi.org/10.1029/2002JD002670>.
13
14

15 Rose, K.A. et al., 2015. Demonstration of a fully-coupled end-to-end model for small pelagic
16 fish using sardine and anchovy in the California Current. *Progress in Oceanography* 138
17 (PB), 348–380. <http://dx.doi.org/10.1016/j.pocean.2015.01.012>.
18
19

20 Rykaczewski, R.R., Dunne, J.P., 2010. Enhanced nutrient supply to the California Current
21 Ecosystem with global warming and increased stratification in an earth system model.
22 *Geophys. Res. Lett.* 37, L21606, <http://dx.doi.org/10.1029/2010GL045019>.
23
24

25 Sánchez-Garrido, J., Fiechter, J., Rose, K., Werner, C., Curchitser, E. 2020. Dynamics of
26 anchovy and sardine populations in the Canary Current off NW Africa: responses to
27 environmental and climate forcing in a climate-to-fish ecosystem model. *Fisheries in
28 Oceanography*. Under Revision.
29
30
31

32 Schwing, F.B., Palacios, D.M., Bograd, S.J., 2005. El Niño impacts on the California
33 Current ecosystems. *U.S. CLIVAR Newslett.* 3 (2), 5–8.
34
35

36 Seo, H., A. J. Miller and J. R Norris, 2016: Eddy-wind interaction in the California Current
37 System: Dynamics and impacts. *Journal of Physical Oceanography*, **46**, 439-459.
38
39

40 Shchepetkin, A.F., McWilliams, J.C., 2005. The regional oceanic modeling system (ROMS):
41 a split-explicit, free-surface, topography-following-coordinate ocean model.
42 *OceanModel*. 9, 347–404.
43
44

45 Stock, C.A., John, J.G., Rykaczewski, R.R., Asch, R.G., Cheung, W.W.L., Dunne, J.P.,
46 Friedland, K.D., Lam, V. W.Y., Sarmiento J.L., Watson R.A., 2017. Reconciling fisheries
47 catch and ocean productivity. *PNAS* 114, E1441–E1449.
48 <https://doi.org/10.1073/pnas.1610238114>.
49
50

51 Thomas, A.C., Strub, P.T., Weatherbee, R.A., James, C., 2012. Satellite views of Pacific
52 chlorophyll variability: Comparisons to physical variability, local versus nonlocal
53 influences and links to climate indices. *Deep-Sea Res. II* 77–80, 99–106.
54
55

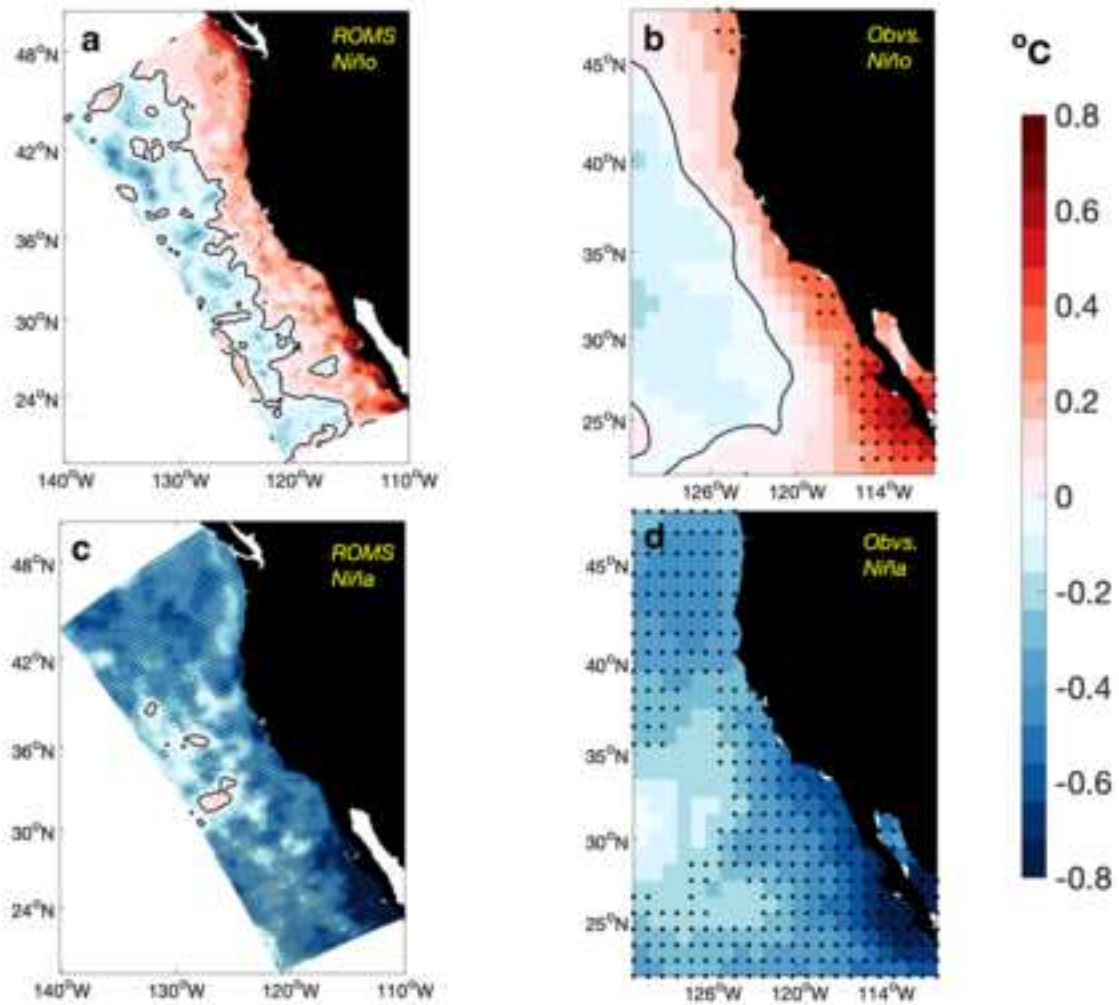
56 Van Oostende, N., Dussin, R., Stock, C.A., Barton, A.D., Curchitser, E., Dunne, J.P., Ward,
57 B.B., 2018. Simulating the ocean's chlorophyll dynamic range from coastal upwelling to
58 oligotrophy. *Progress in Oceanography* 168, 232-247.
59 <https://doi.org/10.1016/j.pocean.2018.10.009>
60
61
62
63
64
65

1
2
3
4
5 Venrick, E.L., 2009. Floral patterns in the California Current: the coastal-offshore
6 boundary zone. *J. Mar. Res.* 67, 89–111
7
8
9
10
11
12
13
14
15
16
17
18
19
20
21
22
23
24
25
26
27
28
29
30
31
32
33
34
35
36
37
38
39
40
41
42
43
44
45
46
47
48
49
50
51
52
53
54
55
56
57
58
59
60
61
62
63
64
65

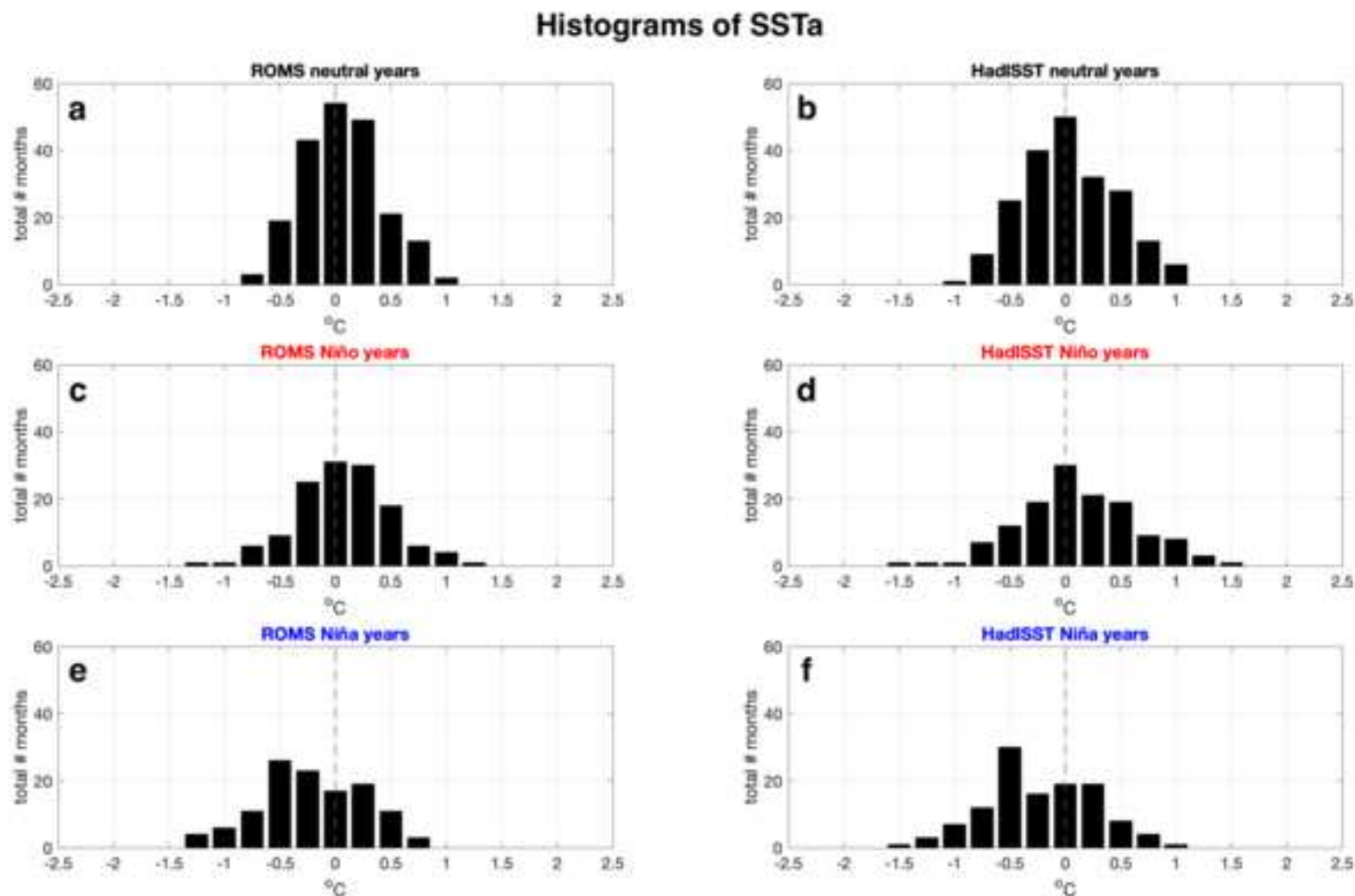
Click here to view linked References

1
2
3
4
5
6
7
8
9
10
11
12
13
14
15
16
17
18
19
20
21
22
23
24
25
26
27
28
29
30
31
32
33
34
35
36
37
38
39
40
41
42
43
44
45
46
47
48
49

Composite DJF-SSTa



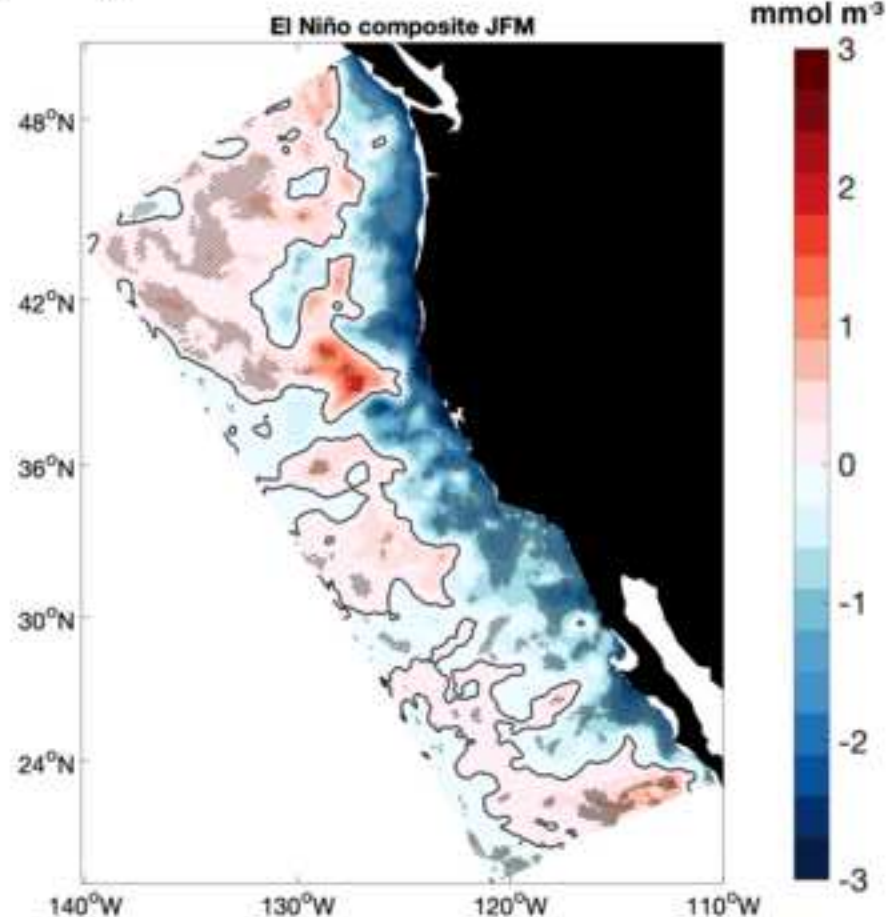
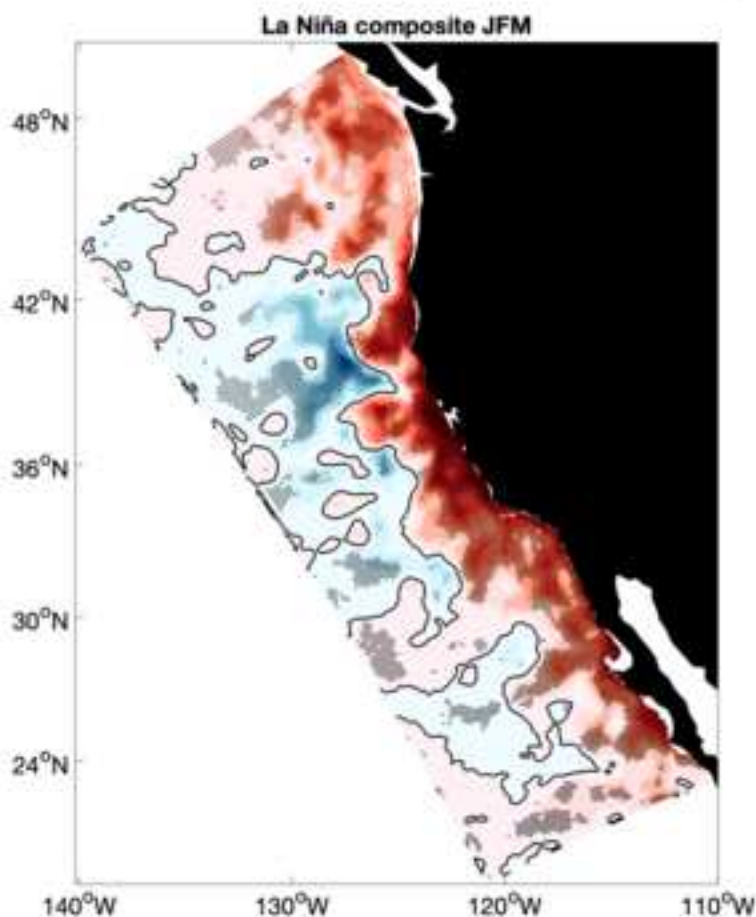
Click here to view linked References



Click here to view linked References

1
2
3
4
5
6
7
8
9
10
11
12
13
14
15
16
17
18
19
20
21
22
23
24
25
26
27
28
29
30
31
32
33
34
35
36
37
38
39
40
41
42
43
44
45
46
47
48
49

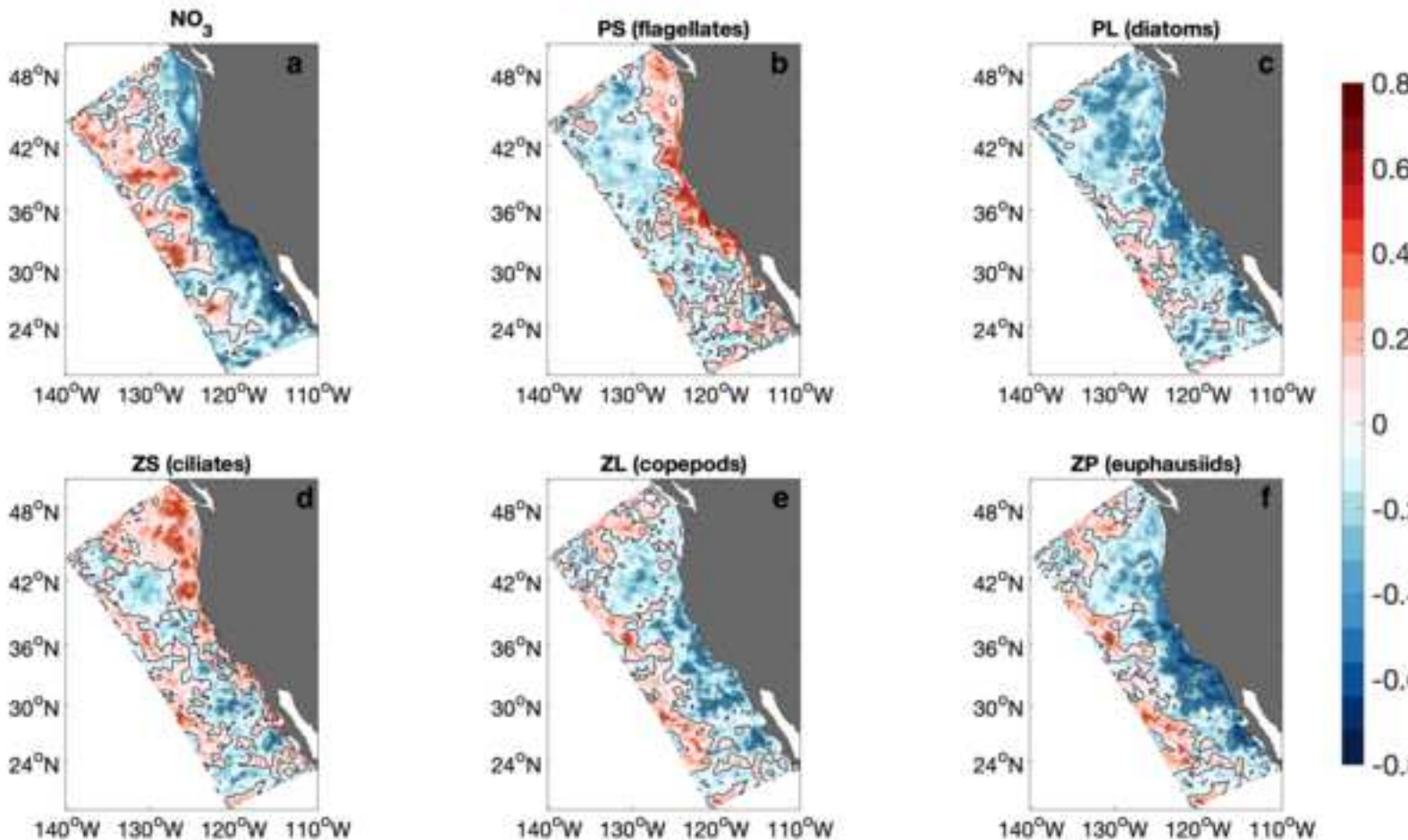
JFM Composite anomalies
vertically averaged NO_3



Click here to view linked References

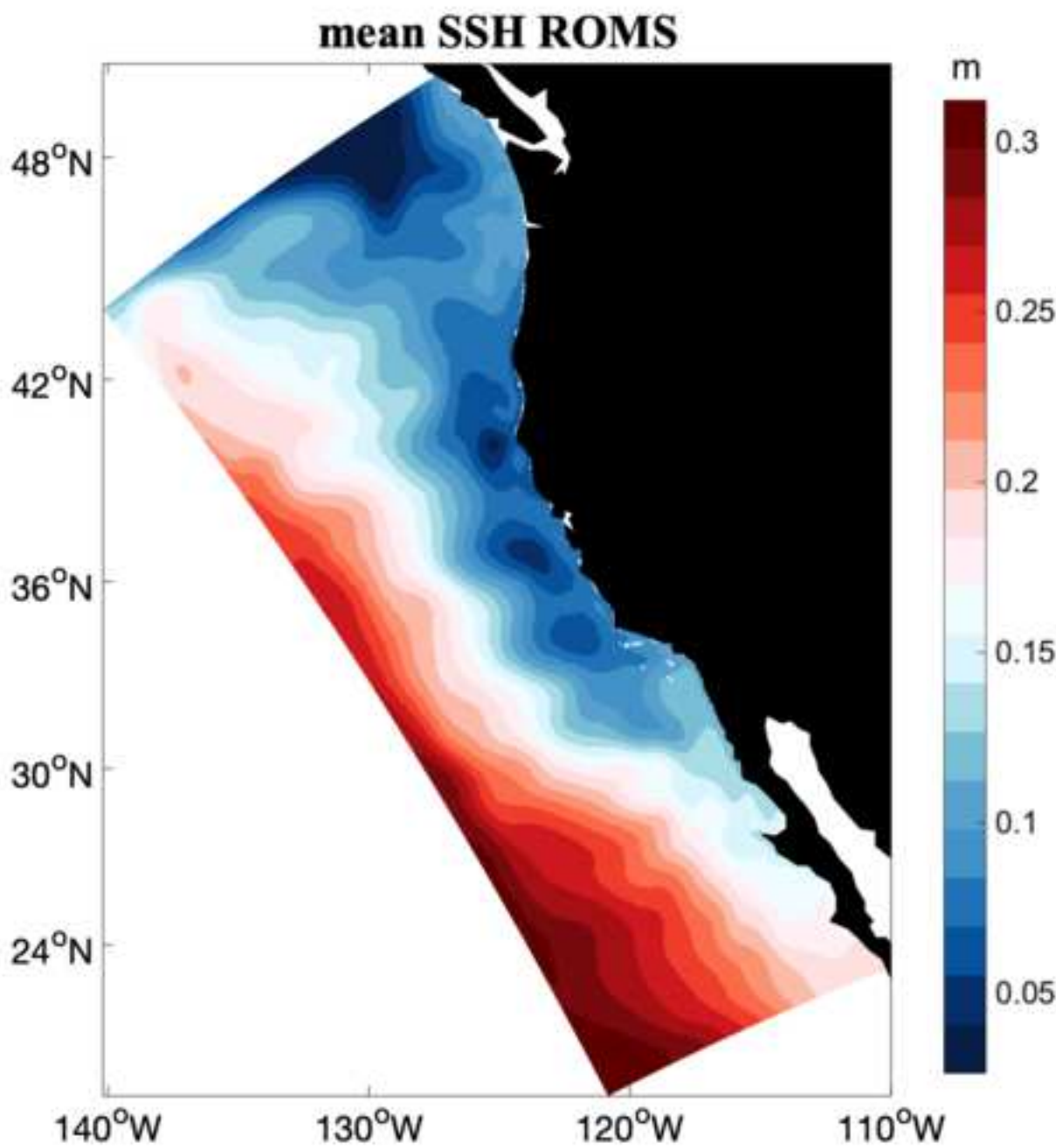
1
2
3
4
5
6
7
8
9
10
11
12
13
14
15
16
17
18
19
20
21
22
23
24
25
26
27
28
29
30
31
32
33
34
35
36
37
38
39
40
41
42
43
44
45
46
47
48
49

lagged correlation at 3 months with ONI-January
NEMURO

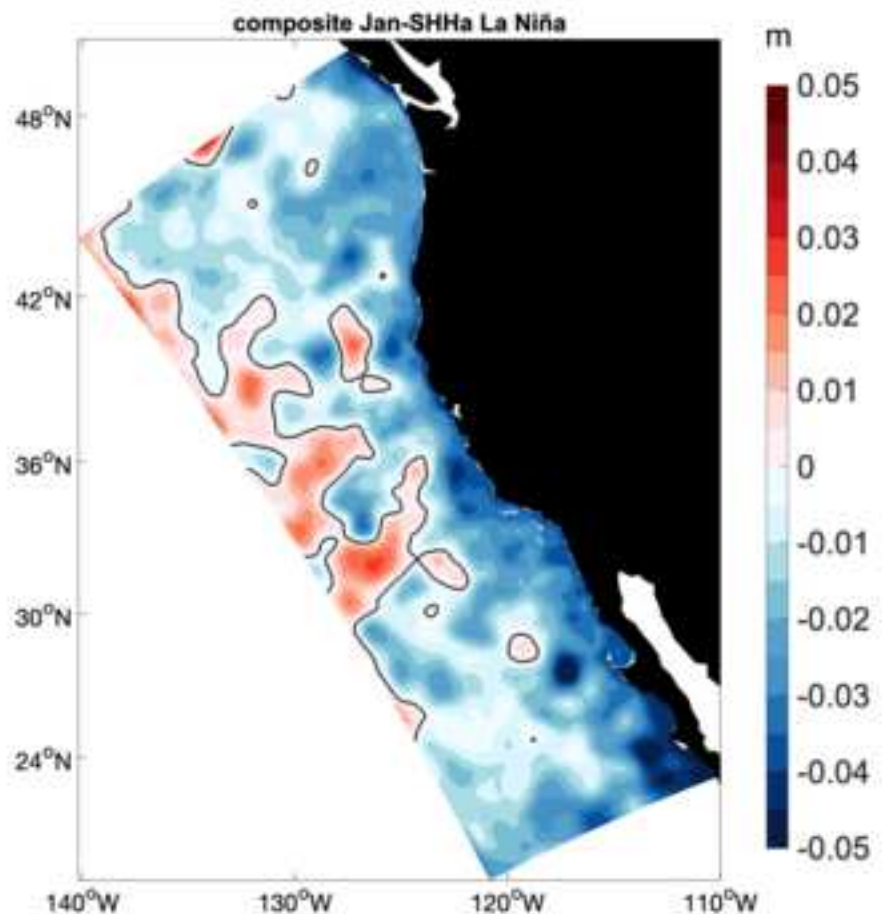
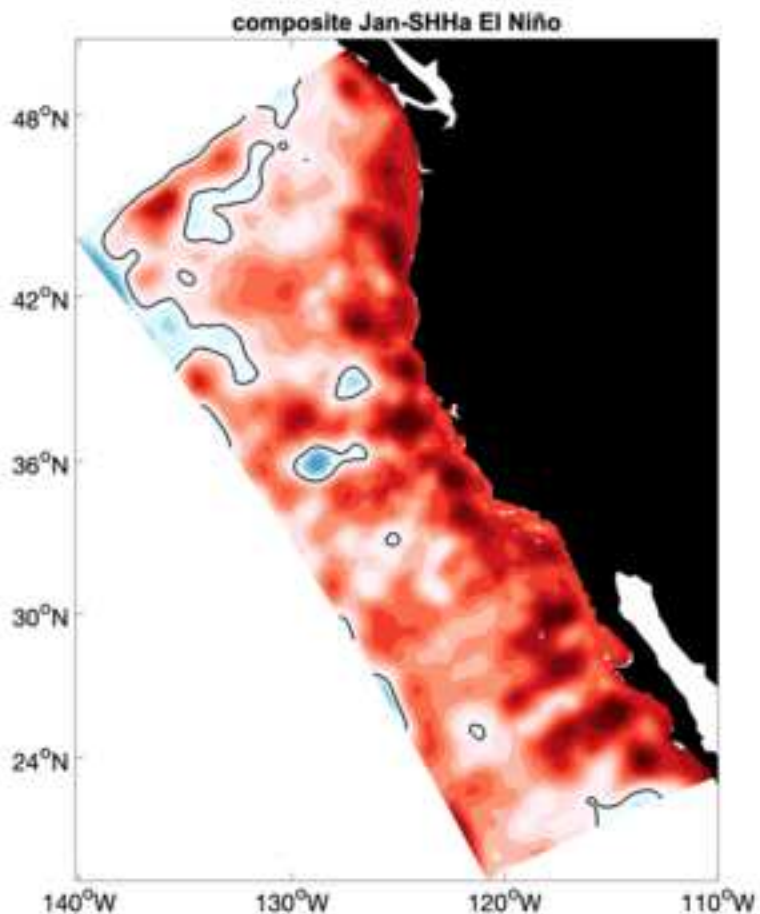


[Click here to view linked References](#)

1
2
3
4
5
6
7
8
9
10
11
12
13
14
15
16
17
18
19
20
21
22
23
24
25
26
27
28
29
30
31
32
33
34
35
36
37
38
39
40
41
42
43
44
45
46
47
48
49
50
51
52
53
54
55
56
57
58
59
60
61
62
63
64
65



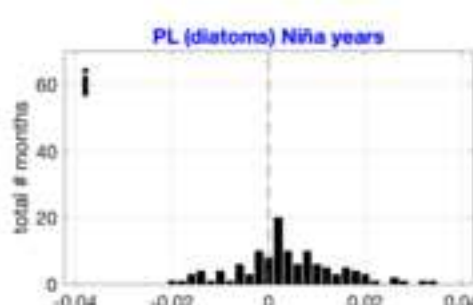
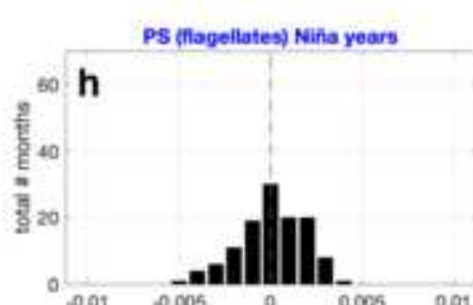
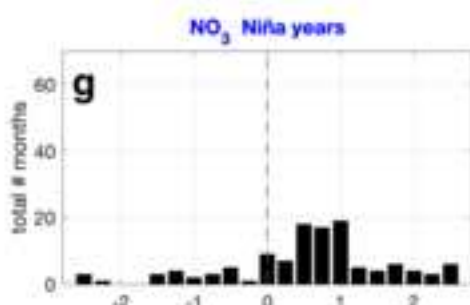
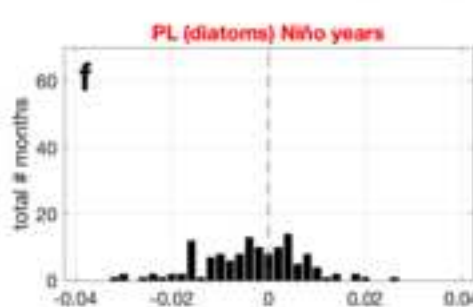
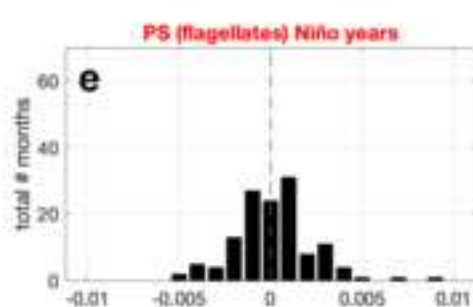
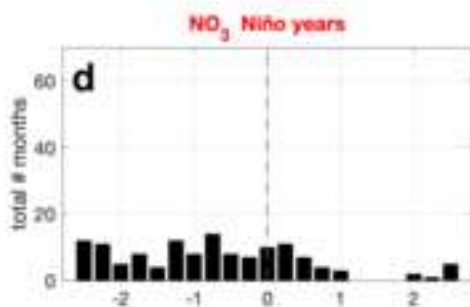
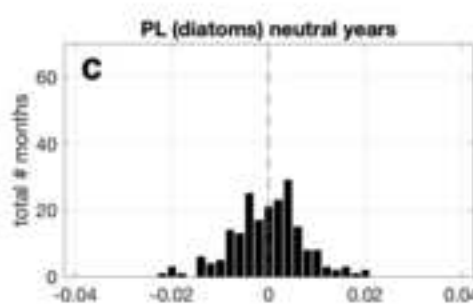
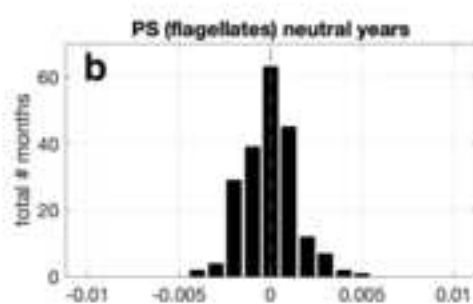
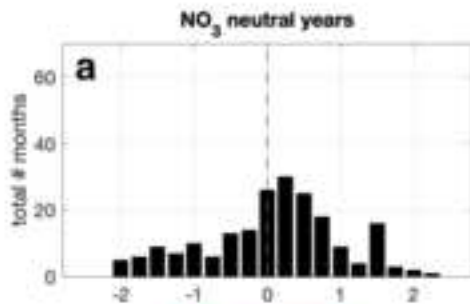
Click here to view linked References



Click here to view linked References

1
2
3
4
5
6
7
8
9
10
11
12
13
14
15
16
17
18
19
20
21
22
23
24
25
26
27
28
29
30
31
32
33
34
35
36
37
38
39
40
41
42
43
44
45
46
47
48
49

Ecological histograms-NEMURO



Click here to view linked References

1
2
3
4
5
6
7
8
9
10
11
12
13
14
15
16
17
18
19
20
21
22
23
24
25
26
27
28
29
30
31
32
33
34
35
36
37
38
39
40
41
42
43
44
45
46
47
48
49

Ecological histograms-NEMURO zooplankton groups

